Novel Heterobimetallic Compounds with Metal−Metal Bonds: The Use of Quinolyl-Substituted Metallocenes as Tridentate Ligands†

Markus Enders,* Gerald Kohl, and Hans Pritzkow

Anorganisch-Chemisches Institut, Universität Heidelberg, Im Neuenheimer Feld 270, D-69120 Heidelberg, Germany

Received October 30, 2001

1,1′-Bis(quinolyl)ferrocene (**1**) and 1,1′-bis(quinolyl)ruthenocene (**2**) were prepared by palladium-catalyzed cross-coupling of zincated metallocenes ($(C_5H_4ZnCl)_2M$; M = Fe, Ru) with 8-bromoquinoline. Both complexes can serve as tridentate ligands toward d^{10} metal ions. Their reactions with anhydrous zinc chloride or with tetrakis(acetonitrile)copper(I) tetrafluoroborate lead to the bimetallic complexes **3**−**6**, in which the zinc or copper ion is coordinated in a tridentate manner by the metallocene derivative **1** or **2**, respectively. Two different coordination modes of the ligands **1** and **2** were observed, both with a metal−metal bond as proved by X-ray analysis. The bond distances Fe−Zn in **3** and Ru−Zn in **4** are practically identical (2.56 Å); the Ru−Cu bond in **6** is somewhat longer (2.63 Å). Whereas the zinc adducts **3** and **4** contain the metallocene ligand in a C_s-symmetric arrangement with a 4-fold-coordinated Zn atom, the Ru−Cu compound **6** has a C_2 symmetry with a 3-fold-coordinated Cu atom. The heterobimetallic compounds **3** and **4** are the first structurally characterized ferrocene and ruthenocene derivatives containing a metal to zinc bond. The complexes **5** and **6** are, to the best of our knowledge, the first examples of adducts of ferrocene and ruthenocene derivatives with copper.

Downloaded by CARLI CONSORTIUM on June 29, 2009
Published on February 22, 2002 on http://pubs.acs.org | doi: 10.1021/om010937o

Introduction

Electrophilic substitution is an important reaction for the synthesis of ferrocene derivatives. Mechanistic investigations have shown that the electrophile may attack the cyclopentadienyl carbon atom from the exo or endo position relative to the metal center.[1] If strong, Lewis acidic electrophiles are used, an interaction with the nonbonding e_{2g} electrons of ferrocene becomes possible and the iron atom serves as a donor. Already in 1960, this basicity of ferrocene and ruthenocene was revealed by their reactivity toward protons and metal-protonated ferrocene was detected by NMR spectroscopy.[2] Adducts of other Lewis acids with ferrocene or ruthenocene were described only in a few cases. X-ray structure analyses exist from adducts of ruthenocene with $HgCl_2$ as well as from adducts of [2]ferrocenophane with $HgCl_2$.[3] With the stronger Lewis acidic boron halides the ring substitution dominates to form ferrocenyl boron dihalides.[4] Zinc dichloride does not react with ferrocene itself but with [2]ferrocenophane, in which the basicity of the iron atom is increased by the inclination of the cyclopentadienyl rings. The existence of an iron−zinc interaction was revealed by Mössbauer spectroscopy.[5] However, no structural characterization of such compounds with metal−zinc bonds have been reported until now.[6] The syntheses of other heterobimetallic metallocene derivatives with a metal−metal bond could be achieved by the use of functionalized cyclopentadienyl ligands containing a phosphorus or sulfur donor group directly bonded to the five-membered ring.[7] Adducts of ferrocene, ruthenocene, and its derivatives with copper are hitherto unknown.

We hereby report on the synthesis and structural investigation of heterobimetallic compounds with metal−metal bonds by the use of quinolyl-substituted metallocene derivatives.

Results

Recently we reported the synthesis of bis[η^5-(8-quinolyl)cyclopentadienyl]iron(II) (**1**) through palladium-catalyzed Negishi cross-coupling (Scheme 1).[8] In an analogous reaction bis[η^5-(8-quinolyl)cyclopentadienyl]-ruthenium(II) (**2**) was prepared from 1,1′-bis(chlorozinc)-ruthenocene and 8-bromoquinoline in the presence of 5 mol % of in situ generated bis(triphenylphosphine)-palladium(0).

† Dedicated to Professor Robert J. P. Corriu.

(1) Cunningham, A. F., Jr. *Organometallics* **1997**, *16*, 1114.
(2) (a) Curphey, T. J.; Santer, J. O.; Rosenblum, M.; Richards, J. H. *J. Am. Chem. Soc.* **1960**, *82*, 5249. (b) Rosenblum, M.; Santer, J. O.; Howells, W. G. *J. Am. Chem. Soc.* **1963**, *85*, 1450.
(3) Watanabe, M.; Nagasawa, A.; Sato, M.; Motoyama, I.; Takayama, T. *Bull. Chem. Soc. Jpn.* **1998**, *71*, 1071.
(4) Ruf, W.; Fueller, M.; Siebert, W. *J. Organomet. Chem.* **1974**, *64*, C45.
(5) Sano, H.; Watanabe, M.; Motoyama, I. *Hyperfine Interact.* **1986**, 833.
(6) (a) Cambridge Stuctural Database, Entries until August 2001. (b) Allen, F. H.; Kennard, O. *Chem. Design Automation News* **1993**, *8*, 31.
(7) (a) Takemoto, S.; Kuwata, S.; Nishibayashi, Y.; Hidai, M. *Inorg. Chem.* **1998**, *37*, 6428. (b) Sato, M.; Suzuki, K.; Asano, H.; Sekino, M.; Kawata, Y.; Habata, Y.; Akabori, S. *J. Organomet. Chem.* **1994**, *470*, 263 and references cited therein.
(8) Enders, M.; Kohl, G.; Pritzkow, H. *J. Organomet. Chem.* **2001**, *622*, 66.

10.1021/om010937o CCC: $22.00 © 2002 American Chemical Society
Publication on Web 02/22/2002

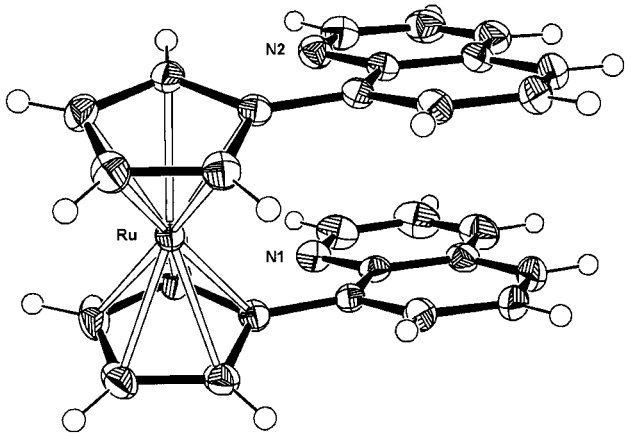

Figure 1. Solid-state structure of **2**. The Ru−Cp(best plane) distance is 1.81 Å.

Scheme 1. Preparation of the Quinolyl-Substituted Metallocenes 1 and 2

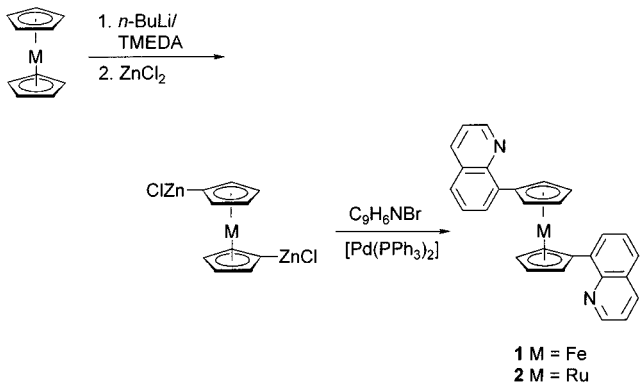

The X-ray structure analysis of **2** (Figure 1) shows that the angles between the cyclopentadienyl and the quinolyl planes are 20.1 and 22.8°, respectively. The geometry of the ruthenocene framework and the two quinolyl groups is eclipsed. The distances between the nearly parallel lying quinolyl substituents are in the range of 3.35 to 3.58 Å. Related arrangements with parallel aromatic groups were found in the solid-state structure of **1**[8] and of 1,1′,3,3′-tetraphenylferrocene.[9] This stacking of the aromatic groups could not be revealed in solution. The ^{1}H NMR spectrum of **2** shows two pseudotriplets for the Cp protons which are typical for AA′BB′ spin systems in monosubstituted cyclopentadienyl derivatives. Therefore, the molecule is fluxional in solution and thus average signals are detected. This fluxionality persists down to a temperature of −100 °C (500.13 MHz ^{1}H NMR spectrum).

Reactivity of 1 and 2 toward Lewis Acids. Treatment of the metallocene derivatives **1** and **2** with 2 equiv of anhydrous zinc dichloride leads to the formation of the heterobimetallic complexes **3** and **4** (Scheme 2). The elemental analyses show that the ratio between the metallocene derivative and zinc dichloride is 1:2. In the FAB$^+$ mass spectra the adducts [**1**ZnCl]$^+$ and [**2**ZnCl]$^+$, respectively, are found.

Crystals of **3** and **4** suitable for X-ray investigations were grown from solutions of **1** and **2**, respectively, in dichloromethane to which anhydrous zinc dichloride was added. The compounds **3** and **4** have very similar geometries. A superposition of the two solid-state structures is shown in Figure 2. The compounds consist of the dianion $[Zn_2Cl_6]^{2-}$ and the complex cation [**1**ZnCl]$^+$ or [**2**ZnCl]$^+$, respectively. In these cations the zinc atoms have a distorted-tetrahedral coordination sphere consisting of the two nitrogen atoms of the quinolyl moieties and one chlorine atom; the fourth position is occupied by an iron atom in **3** or a ruthenium atom in **4**, respectively.

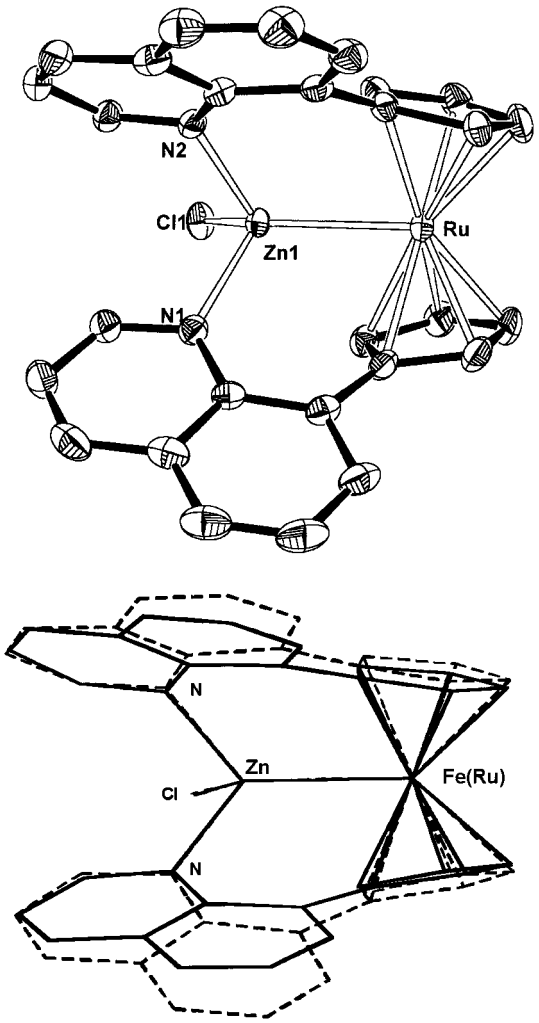

Figure 2. (top) Solid-state structure of the complex cation in **4**. (bottom) Overlay of the complex cations in **3** (—) and **4** (- - -). The counterion $[Zn_2Cl_6]^{2-}$ and the H atoms are omitted for clarity. For selected bond lengths and angles see Table 1.

Due to the metal−zinc interaction the cyclopentadienyl rings are no longer parallel but form an angle of 17.9° (**3**) or 19.1° (**4**) (Table 1). The quinolyl systems deviate somewhat from planarity, the nitrogen atoms showing the largest deviation from the best planes (0.10 Å in **3** and 0.09 Å in **4**) so that the N atoms can better coordinate the zinc ions. The N−Zn distances lie in the range of 2.08−2.12 Å and are consequently slightly longer than in pyridine−zinc coordination compounds.[10]

(9) Schumann, H.; Lentz, A.; Weimann, R. *J. Organomet. Chem.* **1995**, *487*, 245.

(10) Examples for zinc−pyridine coordination compounds: (a) Hennig, C.; Hallmeier, K.-H.; Zahn, G.; Tschwatschal, F.; Hennig, H. *Inorg. Chem.* **1999**, *38*, 38. (b) Doerrer, L. H.; Lippard, S. J. *Inorg. Chem.* **1997**, *36*, 2554. (c) Steffen, W.; Palenik, G. J. *Acta Crystallogr.* **1976**, *B32*, 298.

Downloaded by CARLI CONSORTIUM on June 29, 2009
Published on February 22, 2002 on http://pubs.acs.org | doi: 10.1021/om010937o

Scheme 2. Formation of the Metallocene Complexes 3−6

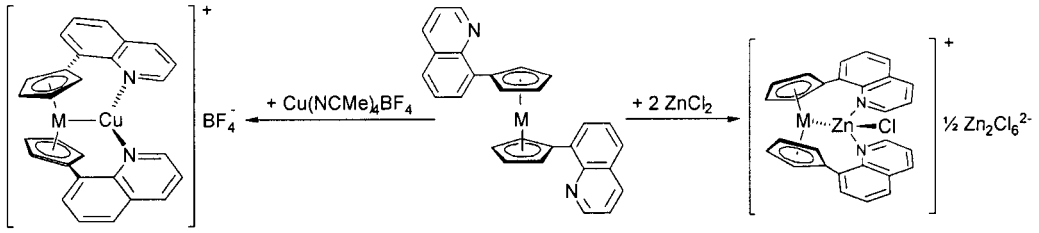

5 M = Fe
6 M = Ru

1 M = Fe
2 M = Ru

3 M = Fe
4 M = Ru

Table 1. Selected Bond Lengths (Å) and Angles (deg) for 3, 4, and 6[a]

	3 (M = Fe, M′ = Zn)	**4** (M = Ru, M′ = Zn)	**6** (M = Ru, M′ = Cu)
M−M′	2.562(1)	2.561(1)	2.634(1)
			2.633(1)
N1−M′	2.122(1)	2.094(2)	1.974(2)
			1.968(2)
N2−M′	2.079(1)	2.101(2)	1.975(2)
			1.961(2)
M′−Cl1	2.231(1)	2.241(1)	
M−Cp[b]	1.67	1.83	1.83
			1.83
M−M′−N1	109.3(1)	111.9(1)	111.2(1)
			110.4(1)
M− M′−N2	113.4(1)	114.2(1)	110.2(1)
			111.7(1)
N1− M′−N2	91.3(1)	96.2(1)	138.5(1)
			137.9(1)
M− M′−Cl1	123.9(1)	123.8(1)	
N1− M′−Cl1	105.5(1)	101.9(1)	
N2− M′−Cl1	108.4(1)	104.9(1)	
Cp−M−Cp	163.7	164.0	174.6
			174.6

[a] For **6** the values for both independent molecules in the unit cell are given. [b] Shortest distance between the plane defined by the Cp-ring and the metal atom.

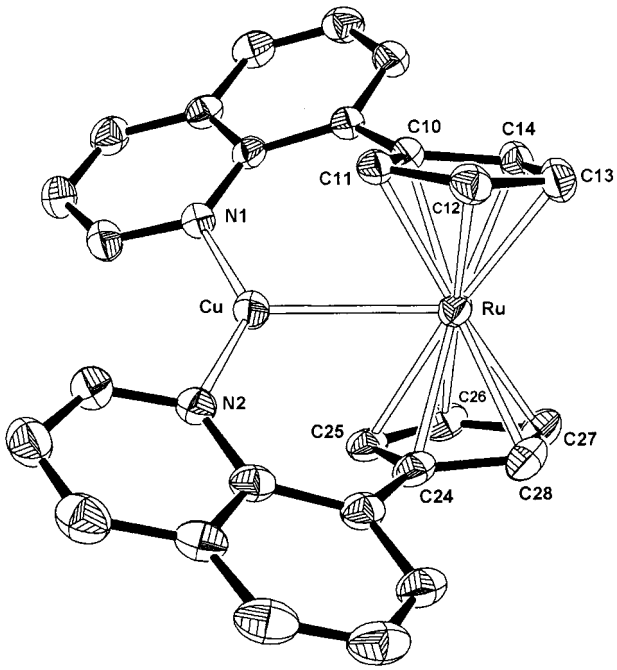

Figure 3. Solid-state structure of the complex cation in **6**. The counterion and the H atoms are omitted for clarity. For selected bond lengths and angles see Table 1.

A reasonable Fe−Zn single-bond length was estimated to be 2.56 Å,[11b] which is in good agreement with the found iron−zinc distance in **3** (2.562(1) Å). However, iron−zinc distances described in the literature are normally significantly shorter (2.32−2.50 Å);[11] only in the cases of [(bpy)ZnFe(CO)$_4$] (2.585 Å)[12] and Zn[FeCp-(CO)$_2$]$_3^-$ (2.564 Å)[13] were longer bonding distances found. The iron−zinc distance in **3** (2.562(1) Å) is nearly identical with the ruthenium−zinc distance in **4** (2.561(1) Å). Compounds with ruthenium−zinc bonds are very rare, and only one compound, a Ru^0−ZnCl$_2$ adduct with a chelating pyridyl−phosphine ligand (with an Ru−Zn distance of 2.659(1) Å), has been characterized by X-ray diffraction so far.[14] The ruthenium−zinc bond in **4** is 0.10 Å shorter than in the published compound. The metal−zinc distances in **3** and **4** are identical, although ruthenium is considerably larger than iron. This is due to the rigid geometry of the tridentate metallocene ligand which defines the coordination cavity.

Since complexation of Zn^{2+} ions with the metallocenes **1** and **2** was successful, the isoelectronic Cu$^+$ ion, which has the same covalent radius (0.74 Å, coordination number 4),[15] should generate similar adducts. Indeed, treatment of **1** and **2** with tetrakis(acetonitrile)copper(I) tetrafluoroborate led to the formation of the heterobimetallic complexes **5** and **6**, respectively. The FAB$^+$ mass spectra show the existence of adducts of the metallocene derivatives with a copper ion. As the metallocenes **1** and **2** serve as tridentate ligands, the coordination sphere of the copper atom might be completed by an acetonitrile ligand. However, the elementary analyses prove that no acetonitrile is contained in the complexes **5** and **6**.

Crystals of the ruthenium−copper complex **6** suitable for an X-ray investigation were grown from a solution of **6** in dichloromethane by diffusion of diethyl ether followed by hexane. The compound crystallizes in the monoclinic space group $P2_1/c$ with two independent molecules in the asymmetric unit, which are very similar. Therefore, only the values of the molecule shown in Figure 3 are discussed.

(11) (a) Fuhr, O.; Fenske, D. *Z. Anorg. Allg. Chem.* **2000**, *626*, 1822. (b) Pierpont, C. G.; Sosinsky, B. A.; Shong, R. G. *Inorg. Chem.* **1982**, *21*, 3247. (c) Burlitch, J. M.; Hayes, S. E.; Whitewell, G. E., II. *Organometallics* **1982**, *1*, 1074.

(12) Neustadt, R. J.; Cymbaluk, T. H.; Ernst, R. D.; Cagle, F. W. *Inorg. Chem.* **1980**, *19*, 2375.

(13) Petersen, R. B.; Ragostan, J. M.; Whitwell, G. E., II; Burlitch, J. M. *Inorg. Chem.* **1983**, *22*, 3407.

(14) Chan, W.-H.; Zhang, Z.-Z.; Mak, T. C. W.; Che, C.-M. *J. Chem. Soc., Dalton Trans.* **1998**, 803.

(15) Holleman, A. F.; Wiberg, E. *Lehrbuch der anorganischen Chemie*, 101st ed.; de Gruyter: Berlin, New York, 1995; p 1838.

Downloaded by CARLI CONSORTIUM on June 29, 2009
Published on February 22, 2002 on http://pubs.acs.org | doi: 10.1021/om010937o

Downloaded by CARLI CONSORTIUM on June 29, 2009
Published on February 22, 2002 on http://pubs.acs.org | doi: 10.1021/om010937o

In contrast to the 4-fold-coordinated zinc ions in **3** and **4**, the copper atom in **6** is coordinated by only three ligands. The nitrogen atoms of the two quinolyl groups and the ruthenium atom surround the Cu^+ ion in a trigonal-planar manner. Therefore, the arrangement of the quinolyl substituents in **6** leads to a chiral molecule with C_2 symmetry. Because of the centrosymmetric space group, the corresponding enantiomer is present in the unit cell. The Cu^+ ion lies nearly exactly in the plane defined by N1, N2, and Ru (deviation 0.01 Å). The ruthenium−copper bond length is, at 2.634(1) Å, in the same range as the corresponding distances in other copper−ruthenium compounds.[16] The angle between the cyclopentadienyl planes is 7.6°; thus, the ruthenocene framework in **6** is less bent than in the Ru−Zn compound **4**.

As seen above, the metallocene derivatives **1** and **2** have three basic centers: the two nitrogen atoms and the metal atom. Treatment of **1** and **2**, respectively, with a solution of hydrochloric acid in diethyl ether leads to the complexes **7** and **8**, in which both nitrogen atoms are protonated. The positive charges of the resulting dications probably inhibit further attack of a third proton at the metal atom with its weaker basicity. The formation of the dications goes ahead with a change of colors from red (**1**) to violet (**7**) and from yellow (**2**) to orange (**8**).

Crystals of the protonated ruthenium complex **8** suitable for X-ray investigations were grown from a solution in dichloromethane (Figure 4). The arrangement of the two protonated quinolyl groups is related to that in the Ru−Cu complex **6**. The N−H functions build hydrogen bridges to one chloride ion, which are shown by the N···Cl distances (N1−Cl1 = 3.14 Å, N2−Cl1 = 3.15 Å).[17] The cyclopentadienyl rings are inclined by 6.0° because of steric interactions with one counterion (Cl1).

As we did not obtain suitable crystals of compound **7**, the analogous compound **7a** was prepared from **1** and trifluoroacetic acid (Figure 5). Again, both nitrogen atoms are protonated. The solid-state structure shows an arrangement different from that of **8**. The two N−H functions interact with two trifluoroacetate anions. The quinolyl groups lie nearly parallel to each other (about 2.8° deviation), and the homocyclic parts are stacked with a distance between the two rings of about 3.5 Å. This arrangement leads to a good separation of the positively charged N−H functions (6.67 Å).

Spectroscopic Investigations and Redox Behavior. The bimetallic compounds **3** and **4** possess C_s symmetry and **6** has C_2 symmetry in the solid state. If these geometries are also present in solution, four signals would be expected for the C−H groups of the Cp rings in the ^{1}H NMR and ^{13}C NMR spectra.

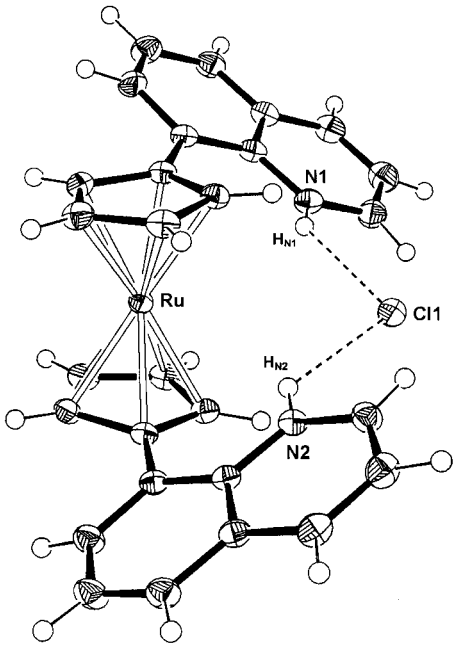

Figure 4. Solid-state structure of **8**. One of the two chloride ions present in the asymmetric unit is not shown. Selected bond lengths (Å) and angles (deg): N1−Cl1 = 3.138(2), N2−Cl1 = 3.148(2), H_{N1}−Cl1 = 2.49(3), H_{N2}−Cl1 = 2.50(3), Ru−Cp(best plane) = 1.82, Ru−C_{Cp} = 2.166(2)−2.203(2); Cp−Ru−Cp = 175.6.

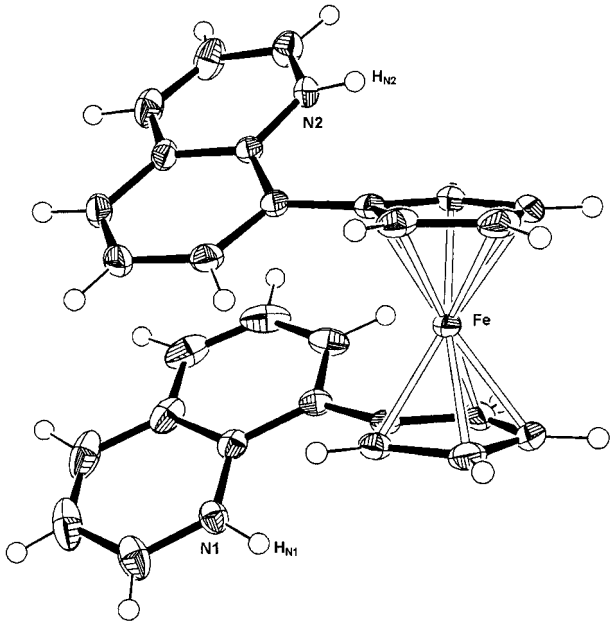

Figure 5. Solid-state structure of the complex dication in **7a**. The counterions and the two trifluoroacetic acid molecules, present in the asymmetric unit, are omitted. The Fe−Cp(best plane) distance is 1.66 Å.

However, the copper compounds **5** and **6** are fluxional at room temperature, so that only two signals are present. These are split in the ^{1}H NMR spectrum into pseudotriplets, as expected for an AA′BB′ spin system. Therefore, a fast exchange of the positions of the quinolyl groups must occur. In both compounds the signals become broader upon cooling. For compound **5** four well-separated signals appear at −70 °C and below, as expected from the solid-state structure (Figure 6). The coalescence temperature is −58 ± 2 °C. The

(16) See for example: (a) Ellis, D. D.; Couchman, S. M.; Jeffery, J. C.; Malget, J. M.; Stone, F. G. A. *Inorg. Chem*. **1999**, *38*, 1981. (b) Ellis, D. D.; Franken, A.; Stone, F. G. A. *Organometallics* **1999**, *18*, 2362. (c) Beswick, M. A.; Lewis, J.; Raithby, P. R.; de Arellano, M. C. R. *J. Chem. Soc., Dalton Trans.* **1996**, 4033. (d) Gunale, A. S.; Jensen, M. P.; Phillips, D. A.; Stern, C. L.; Shriver, D. F. *Inorg. Chem*. **1992**, *31*, 2622. (e) Deng, H.; Shore, S. G. *Organometallics* **1991**, *10*, 3486. (f) McCarthy, P. J.; Salter, I. D.; Armstrong, K. P.; McPartlin, M.; Powell, H. R. *J. Organomet. Chem*. **1990**, *394*, 711.

(17) Stout, G. H.; Jensen, L. H. *X-ray Structure Determination*: *A Practical Guide*; Macmillan: New York, 1968.

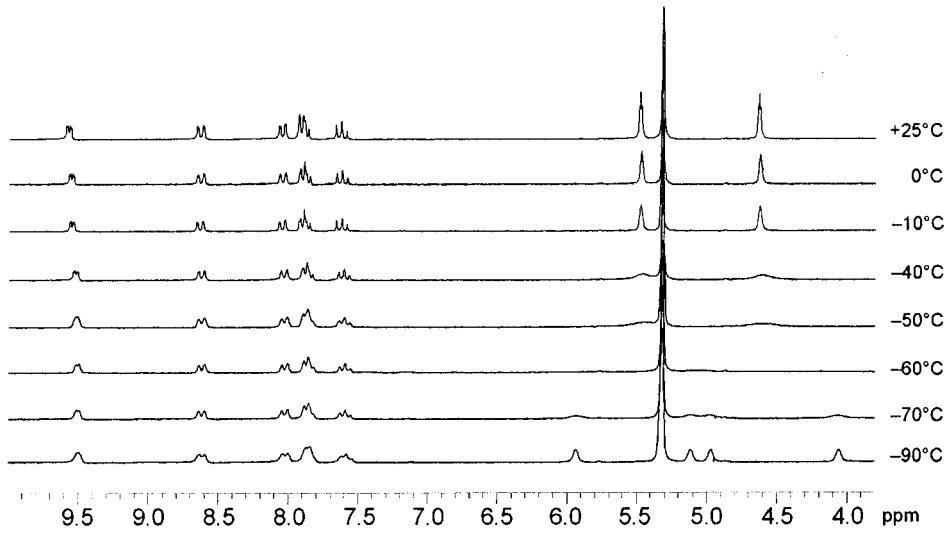

Figure 6. Temperature-dependent dynamic ^{1}H NMR spectra (200.13 MHz, CD_2Cl_2) of **5**.

Downloaded by CARLI CONSORTIUM on June 29, 2009
Published on February 22, 2002 on http://pubs.acs.org | doi: 10.1021/om010937o

coalescence temperature of the Ru−Cu compound **6** is about −98 ± 2 °C.

NMR investigations of the iron−zinc compound **3** were not possible because of low solubility. The ruthenium−zinc compound **4** slightly dissolves in dichloromethane. Addition of tetrabutylammonium hexafluorophosphate strongly increases the solubility of **4**. In addition, the fluxionality changes. Whereas pure **4** in CD_2Cl_2 shows two broadened signals for the Cp protons at room temperature, the mixture with $(n\text{-}Bu_4)NPF_6$ leads to four broadened signals, which sharpen at lower temperature.

The aromatic signals of the quinolyl substituents of **4**−**6** remain almost unchanged upon cooling. The coordination of the Zn and Cu ions, respectively, leads to a characteristic shift of the resonance of the proton adjacent to the nitrogen atom. Whereas this signal appears at about δ 8.8 in the complexes **1** and **2**, it is shifted to approximately δ 9.5 in **4**−**6**.

The redox behavior of ferrocene and ruthenocene has been studied extensively. Whereas the cation $[Cp_2Fe]^+$ is stable, the oxidation of Cp_2Ru leads to an reactive intermediate which is only stable in the presence of a noncoordinating supporting electrolyte.[18] The quinolyl substituents in **1** and **2** lead to a cathodic shift of the oxidation potential of 0.15 V (**1** vs Cp_2Fe) and 0.48 V (**2** vs Cp_2Ru), respectively. This effect is well-known and can be explained by the +I effect of the substituents, which stabilizes the positively charged complex cations.

The interaction between the metallocene units and the coordinated ions was investigated by cyclic voltammetric measurements (Table 2). The zinc compound **3** possesses a solubility too low for cyclic voltammetric measurements; **4** shows a very broad and uncharacteristic oxidation wave beginning at +0.5 V. The cyclic voltammograms of the copper compounds **5** and **6** reveal more pieces of information. Oxidation occurs at higher potential compared to **1** and **2**. The anodic shifts are 0.56 V (**5** vs **1**) and 0.50 V (**6** vs **2**), respectively. These values are large compared to the anodic shifts in crown ether functionalized ferrocene derivatives.[19] This is not surprising; hence, the influence of the positive charged copper ion on the oxidation potential of iron and ruthenium, respectively, is dependent on the metal−metal distance. Siemeling et al. reported an anodic shift of 0.46 V for a ferrocene−copper(I) compound where the two metal atoms have a distance of 3.23 Å.[20] In this compound, the Cu(I)−Cu(II) oxidation was detected as a broad peak at about 0.9 V. We assume that the metallocene-centered oxidations in the copper compounds **5** and **6** at about 1.0 V are accompanied by Cu(I)−Cu(II) oxidations. This suggestion is supported by the occurrence of a shoulder in the broad oxidation peak of **6**. The oxidation potentials of **7** and **5** are nearly identical, although the cation in **7** bears two positive charges, whereas in **5** it is only a monocation. The directly bonded Cu^+ ion increases the redox potential of the ferrocene moiety as much as two H^+ ions which

Table 2. Electrode Potentials for the Metallocene-Centered Oxidation Processes[a]

	$E_{p,a}$	$E_{p,c}$	$E_{1/2}$(rev)
Cp_2Fe	+0.51	+0.43	+0.47
Cp_2Ru	+1.18		irrev[b]
1	+0.36	+0.29	+0.33
2	+0.70	+0.40	*c*
4	broad uncharacteristic oxidation wave beginning at about +0.5		irrev
5	+0.92[d]	+0.64	*c*
6	+1.2 (broad, shoulder at +1.05)[d]	+0.37[e]	irrev
7	+0.85	+0.70	+0.78
8	broad uncharacteristic oxidation wave beginning at about +0.7		irrev

[a] In V vs SCE. $E_{p,a}$ = anodic peak potential; $E_{p,c}$ = cathodic peak potential. [b] With tetrabutylammonium tetrakis[3,5-bis(trifluoromethyl)phenyl]borate as supporting electrolyte; reversible oxidation with $E_{1/2}$ = +1.03 V.[18] [c] Only partly reversible, $i_{p,a} > i_{p,c}$. [d] Probably also Cu(I)−Cu(II) oxidation. [e] Reaction product of irreversible oxidation at +1.2 V.

(18) Hill, M. G.; Lamanna, W. M.; Mann, K. R. *Inorg. Chem.* **1991**, *30*, 4687.

(19) Plenio, H.; Aberle, C.; Al Shihadeh, Y.; Lloris, J. M.; Martínez-Máñez, R.; Pardo, T.; Soto, J. *Chem. Eur. J.* **2001**, *7*, 2848.

(20) Neumann, B.; Siemeling, U.; Stammler, H.-G.; Vorfeld, U.; Delis, J. G. P.; van Leeuwen, P. W. N. M.; Vrieze, K.; Fraanje, J.; Goubitz, K.; de Biani, F. F.; Zanello, P. *J. Chem. Soc., Dalton Trans.* **1997**, 4705.

are further apart from the redox-active center. Irreversible reductions occur at potentials between −0.7 and −1.0 V for the complexes **4**−**8**. As the metallocenes **1** and **2** could not be reduced up to −2.0 V, we assume that these cathodic processes of **4**−**8** are due to the reduction of Zn^{2+}, Cu^{+}, and H^{+}, respectively.

Conclusion

Quinolyl-substituted ferrocenes and ruthenocenes are able to bind Lewis acidic metal cations such as Zn^{2+} and Cu^{+} via the two nitrogen donor atoms. In addition the iron or ruthenium atom, respectively, serves as a third donor function and completes the coordination sphere of the metal cation. Due to the rigid ligand framework, the iron−zinc complex **3** and the ruthenium−zinc complex **4** have very similar geometries with identical metal−metal distances. The question whether the proximity of the two metal atoms is only a consequence of the geometric prerequisites or whether there is an attractive bond cannot be answered definitely. However, it is known that the nonbonding e_{2g} electrons of metallocenes can interact with Lewis acids; the best known example is Rosenblum's $[Cp_2Fe-H]^{+}$.[2] This fact together with the results obtained by Sano et al.,[5] who isolated ferrocene−zinc adducts with unsupported metal−metal bonds, leads us to the conclusion that the interaction in the compounds **3**−**6** is a donor−acceptor type metal−metal bond.

Experimental Section

All experiments were carried out under an atmosphere of dry argon. Solvents were dried by using standard procedures and distilled prior to use. 8-Bromoquinoline,[21] 1,1′-dilithioruthenocene,[22] and tetrakis(acetonitrile)copper(I) tetrafluoroborate[23] were prepared according to the literature procedures. $ZnCl_2$ was dried by refluxing in thionyl chloride until no evolution of gas was observed.[24] All other reagents were used as purchased. − NMR measurements were carried out on Bruker DRX 200 (200.13 MHz for ^{1}H, 50.32 MHz for ^{13}C, 64.21 MHz for ^{11}B) and Bruker DRX 500 spectrometers (500.13 MHz for ^{1}H); the ^{1}H NMR spectra were calibrated using signals of residual protons from the solvent referenced to $SiMe_4$. The ^{13}C spectral chemical shifts are reported relative to the ^{13}C solvent signals. The ^{11}B NMR spectra were calibrated using $BF_3 \cdot (C_2H_5)_2O$ as an external standard. Variable-temperature measurements were performed with a Bruker BVT 3300 DIGITAL unit. MS measurements were carried out on JEOL JMS-700 and VG ZAB-2F instruments. Cyclic voltammetry used a PAR 263A potentiostat, a METROHM glassy-carbon-disk working electrode, a saturated calomel reference electrode, and dichloromethane solvent with 0.1 mol L^{-1} $(n\text{-}Bu_4)NPF_6$ as supporting electrolyte; the scan rate was 100 mV s^{-1}.

1,1′-Bis(η^5-quinolylcyclopentadienyl)ruthenium(II) (2). 1,1′-Dilithioruthenocene (3.53 g, 15.3 mmol) was dissolved in 80 mL of thf, to which a solution of 4.16 g (30.5 mmol) of $ZnCl_2$ in 40 mL of thf was added slowly; this mixture was stirred for 2 h. In a separate flask $(PPh_3)_2PdCl_2$ (1.07 g, 1.5 mmol) was suspended in 20 mL of thf, to which was added dropwise 3.1 mL (3.1 mmol) of a 1.0 M solution of Dibal-H in thf. This gave a homogeneous dark solution of $(PPh_3)_2Pd$, which was added to the 1,1′-bis(chlorozinc)ruthenocene via a cannula. 8-Bromoquinoline (6.35 g, 30.5 mmol) was added dropwise, and the resulting dark suspension was stirred at room temperature for 1 week. The reaction mixture was quenched by adding a solution of 16.7 g (0.42 mol) of NaOH in 55 mL of water. After 3 h of stirring the organic layer was separated from the water fraction, which was extracted twice with 50 mL of CH_2Cl_2. The combined organic layers were concentrated to about 20 mL, and the yellow precipitate was collected by filtration, washed twice with 50 mL of pentane, and dried under vacuum. Further product can be obtained by filtration of the mother liquor through Al_2O_3/5% H_2O with dichloromethane as eluting agent and storage of the resulting solution at −28 °C: yield 4.34 g (8.94 mmol, 59%); mp 230 °C. ^{1}H NMR ($CDCl_3$, 200.13 MHz): δ 4.76 (pt, 4H), 5.46 (pt, 4H), 6,96 (dd, ^3J(H,H) = 7.5 Hz, ^3J(H,H) = 7.9 Hz, 2H), 7.19 (dd, ^3J(H,H) = 4.3 Hz, ^3J(H,H) = 8.3 Hz, 2H), 7.40−7.52 (m, 4H), 7.94 (dd, ^3J(H,H) = 8.2 Hz, ^4J(H,H) = 1.7 Hz, 2H), 8.76 (dd, ^3J(H,H) = 4.3 Hz, ^4J(H,H) = 1.9 Hz, 2H). ^{13}C NMR ($CDCl_3$): δ 71.8, 74.7 (Cp *C*H); 89.0 (quat C_{Cp}); 120.3, 125.5, 125.6, 129.6, 135.8, 148.8 (quinoline *C*H); 127.6, 128.2, 135.3 (quat $C_{quinoline}$). MS (EI): *m*/*z* (%) 486 (100, M^+), 293 (43, $C_{14}H_9NRu^+$). HR-MS (EI): calcd for $C_{28}H_{20}N_2{}^{102}Ru$ 486.0669, found 486.0681. Anal. Calcd: C, 69.26; H, 4.15; N, 5.77. Found: C, 68.92; H, 4.15; N, 5.80.

(1)$ZnCl^+(Zn_2Cl_6^{2-})_{1/2}$ (3). Anhydrous $ZnCl_2$ (264 mg, 1.94 mg) was added to a solution of **1** (426 mg, 0.97 mmol) in 20 mL of dichloromethane. After the mixture was stirred for 1 week, an orange solid was formed which was separated by filtration, washed with a few milliliters of hexane followed by dichloromethane, and dried under vacuum: yield 670 mg (0.94 mmol, 97%). MS (FAB^+): *m*/*z* (%) 539 (1, (**1**)$ZnCl^+$), 441 (100, (**1**)H^+), 248 (74, $C_{14}H_{10}NFe^+$). HR-MS (FAB^+): calcd for $C_{28}H_{20}N_2Fe^{64}Zn^{35}Cl$ 538.9956, found 538.9943. Anal. Calcd for $C_{28}H_{20}N_2FeZn_2Cl_4 \cdot CH_2Cl_2$ (797.83): C, 43.66; H, 2.78; N, 3.51. Found: C, 43.38; H, 3.15; N, 3.72.

(2)$ZnCl^+(Zn_2Cl_6^{2-})_{1/2}$ (4). Anhydrous $ZnCl_2$ (136 mg, 1.00 mmol) was added to a solution of **2** (243 mg, 0.50 mmol) in 20 mL of toluene. After the mixture was stirred for 10 days, a yellow solid was formed which was separated by filtration, washed with a few milliliters of hexane followed by dichloromethane, and dried under vacuum: yield 358 mg (0.47 mmol, 94%). ^{1}H NMR (CD_2Cl_2, 500.13 MHz, T = 280 K): δ 5.06 (s, 2H), 5.79 (s, 2H), 5.88 (s, 2H), 6.20 (s, 2H), 7.46 (dd, ^3J(H,H) = 7.6 Hz, ^3J(H,H) = 8.0 Hz, 2H), 7.69 (dd, ^3J(H,H) = 5.0 Hz, ^3J(H,H) = 8.0 Hz, 2H), 7.74 (dd, ^3J(H,H) = 8.0 Hz, ^4J(H,H) = 1.3 Hz, 2H), 7.89 (dd, ^3J(H,H) = 7.7 Hz, ^4J(H,H) = 1.3 Hz, 2H), 8.35 (dd, ^3J(H,H) = 8.0 Hz, ^4J(H,H) = 1.7 Hz, 2H), 9.45 (dd, ^3J(H,H) = 5.0 Hz, ^4J(H,H) = 1.7 Hz, 2H). MS (FAB^+): *m*/*z* (%) 587 (100, (**2**)$ZnCl^+$), 551 (29, (**2**)Zn^+ − H), 486 (26, **2**$^+$), 294 (63, $C_{14}H_{10}NRu^+$). HR-MS (FAB^+): calcd for $C_{28}H_{20}N_2{}^{102}Ru^{66}Zn^{35}Cl$ 586.9619, found 586.9641. Anal. Calcd for $C_{28}H_{20}N_2RuZn_2Cl_4$: C, 44.36; H, 2.66; N, 3.70. Found: C, 42.71; H, 3.17; N, 3.11.

(1)$CuBF_4$ (5). $Cu(NCMe)_4BF_4$ (100 mg, 0.32 mmol) was suspended in 30 mL of toluene. Then the ferrocene derivative **1** (140 mg, 0.32 mmol) was added and the reaction mixture was stirred at room temperature for 3 days. The red precipitate that formed was separated from the solution by filtration, washed with a small amount of pentane, and dried under vacuum: yield 179 mg (0.30 mmol, 95%). ^{1}H NMR (CD_2Cl_2, 200.13 MHz): δ 4.63 (pt, 4H), 5.48 (pt, 4H), 7.63 (m, 2H), 7.84−7.96 (m, 4H), 8.05 (dd, ^3J(H,H) = 8.0 Hz, ^4J(H,H) = 1.3 Hz, 2H), 8.63 (dd, ^3J(H,H) = 8.4 Hz, ^4J(H,H) = 1.5 Hz, 2H), 9.58 (dd, ^3J(H,H) = 4.7 Hz, ^4J(H,H) = 1.6 Hz, 2H). ^{13}C NMR ($CDCl_3$): δ 66.4, 73.3 (Cp *C*H); 85.3 (quat C_{Cp}); 122.5, 127.5, 129.7, 133.1, 140.9, 152.3 (quinoline *C*H); 130.7, 131.8, 143.3 (quat $C_{quinoline}$). ^{11}B NMR (CD_2Cl_2): δ −1.3. MS (FAB^+): *m*/*z* (%) 503 (100, (**1**)Cu^+), 248 (74, $C_{14}H_{10}NFe$). Anal. Calcd for $C_{28}H_{20}N_2FeCuBF_4$: C, 56.94; H, 3.41; N, 4.74. Found: C, 53.47; H, 3.42; N, 4.64.

(21) Mirek, J. *Rocz. Chem.* **1960**, *34*, 1599; *Chem. Abstr.* **1961**, *55*, 22314g.
(22) Arnold, R.; Foxman, B. M.; Rosenblum, M.; Euler, W. B. *Organometallics* **1988**, *7*, 1253.
(23) Hathaway, B. J.; Holah, D. G.; Postlethwaite, J. D. *J. Chem. Soc.* **1961**, 3215.
(24) Armarego, W. L. F.; Perrin, D. D. *Purification of Laboratory Chemicals*; Butterworth-Heinemann: Oxford, U.K., 1997; p 452.

Downloaded by CARLI CONSORTIUM on June 29, 2009
Published on February 22, 2002 on http://pubs.acs.org | doi: 10.1021/om010937o

Table 3. Crystal Data and Structure Refinement Details for 2−4, 6, 7a, 8

	2	3	4	6	7a	8
empirical formula	$C_{28}H_{20}N_2Ru$	$C_{29}H_{22}Cl_6FeN_2Zn_2$	$C_{28}H_{20}Cl_4N_2RuZn_2$	$C_{28}H_{20}BCuF_4N_2Ru$	$C_{36}H_{24}F_{12}FeN_2O_8$	$C_{29}H_{24}Cl_4N_2Ru$
fw	485.53	797.78	758.07	635.88	896.42	643.37
cryst syst	monoclinic	triclinic	triclinic	monoclinic	monoclinic	monoclinic
space group	$P2_1/c$	$P\bar{1}$	$P\bar{1}$	$P2_1/c$	$P2_1/n$	$P2_1/n$
unit cell dimens						
a, Å	13.3800(6)	11.0486(1)	9.5003(7)	14.5536(7)	7.0474(4)	9.2043(5)
b, Å	10.1313(5)	11.0908(1)	11.1545(8)	17.9434(9)	20.6909(13)	20.3045(12)
c, Å	14.5490(7)	13.9456(2)	13.6848(9)	17.5653(9)	24.7122(16)	13.8579(8)
α, deg	90	111.469(1)	106.322(1)	90	90	90
β, deg	93.025(1)	105.801(1)	106.151(1)	99.099(1)	93.752(2)	103.0230(10)
γ, deg	90	92.618(1)	90.491(1)	90	90	90
V, Å^3	1969.5(2)	1509.91(3)	1330.9(2)	4529.3(4)	3595.7(4)	2523.3(2)
Z	4	2	2	8	4	4
calcd density, Mg/m^3	1.637	1.755	1.892	1.865	1.656	1.694
abs coeff, mm^{-1}	0.815	2.605	2.772	1.661	0.538	1.068
F(000)	984	796	748	2528	1808	1296
cryst size, mm^3	0.28 × 0.26 × 0.22	0.44 × 0.42 × 0.38	0.38 × 0.16 × 0.07	0.40 × 0.29 × 0.09	0.38 × 0.32 × 0.15	0.27 × 0.14 × 0.14
θ range for data collection, deg	2.45−32.00	1.65−28.29	1.91−32.06	1.82−32.06	1.92−28.28	1.81−32.07
no. of rflns collected	19 566	19 813	23 715	53 129	28 535	23 594
no. of indep rflns (R(int))	6508 (0.0291)	7306 (0.023)	8905 (0.0367)	15 272 (0.0416)	8942 (0.042)	8397 (0.0332)
no. of data/restraints/params	6508/0/360	7306/0/449	8905/0/414	15272/0/827	8942/175/680	8397/3/423
goodness of fit on F^2	1.036	1.044	1.056	1.028	1.030	1.049
final R indices ($I > 2\sigma(I)$)						
R1	0.0271	0.0250	0.0335	0.0354	0.0483	0.0344
wR2	0.0688	0.0664	0.0766	0.0868	0.1178	0.0851
R indices (all data)						
R1	0.0332	0.0272	0.0517	0.0524	0.0709	0.0468
wR2	0.0731	0.0674	0.0871	0.0962	0.1321	0.0947
largest diff peak and hole, e Å^{-3}	1.164 and −0.349	0.500 and −0.457	1.091 and −0.866	1.942 and −0.885	0.690 and −0.476	1.704 and −0.667

Downloaded by CARLI CONSORTIUM on June 29, 2009
Published on February 22, 2002 on http://pubs.acs.org | doi: 10.1021/om010937o

(2)CuBF$_4$ (6). Cu(NCMe)$_4$BF$_4$ (100 mg, 0.32 mmol) was suspended in 30 mL of toluene. Then the ruthenocene derivative **2** (154 mg, 0.32 mmol) was added and the reaction mixture was stirred at room temperature for 3 days. A yellow precipitate formed, which was separated from the solution by filtration, washed with a small amount of hexane, and dried under vacuum: yield 165 mg (0.26 mmol, 81%). ^{1}H NMR (CD_2Cl_2, 200.13 MHz): δ 4.92 (pt, 4H), 5.76 (pt, 4H), 7.64 (t, ^3J(H,H) = 7.8 Hz, 2H), 7.84 (dd, ^3J(H,H) = 4.8 Hz, ^3J(H,H) = 8.3 Hz, 2H), 7.99−8.06 (m, 4H), 8.59 (dd, ^3J(H,H) = 8.4 Hz, ^4J(H,H) = 1.6 Hz, 2H); 9.48 (dd, ^3J(H,H) = 4.8 Hz, ^4J(H,H) = 1.6 Hz, 2H). ^{13}C NMR (CD_2Cl_2): δ 71.4, 74.7 (Cp *C*H); 89.0 (quat C_{Cp}); 122.4, 127.5, 129.6, 133.5, 140.7, 152.2 (quinoline *C*H); 130.6, 131.2, 143.1 (quat $C_{quinoline}$). ^{11}B NMR (CD_2Cl_2): δ −1.3. MS (FAB$^+$): *m*/*z* (%) 549 (100, (**2**)Cu$^+$), 294 (24, $C_{14}H_{10}NRu$). Anal. Calcd for $C_{28}H_{20}N_2RuCuBF_4$: C, 52.89; H, 3.17; N, 4.41. Found: C, 53.16; H, 3.31; N, 4.52.

1(HCl)$_2$ (7). A solution of **1** (100 mg, 0.23 mmol) in 20 mL of dichloromethane was treated with 1 mL of a saturated solution of hydrochloric acid in diethyl ether. The color changed from red to deep violet. After the mixture was stirred for 1 h, the solution was filtered off and the violet residue was washed twice with dichloromethane and dried under vacuum: yield 87 mg (0.17 mmol, 74%). ^{1}H NMR (DMSO-d_6, 200.13 MHz): δ 4.47 (br, 4H), 5.16 (br, 4H), 7.22 (m, 2H), 7.51 (dd, ^3J(H,H) = 3.9 Hz, ^3J(H,H) = 7.9 Hz, 2H), 7.72 (d, ^3J(H,H) = 7.6 Hz, 2H), 7.81 (d, ^3J(H,H) = 7.3 Hz, 2H), 8.43 (d, ^3J(H,H) = 7.7 Hz, 2H), 8.80 (d, ^3J(H,H) = 3.8 Hz, 2H), 11.6 (br, 2H). ^{13}C NMR (DMSO-d_6): δ 70.5, 71.5 (Cp *C*H); 82.8 (quat C_{Cp}); 121.0, 126.3, 127.0, 132.0, 141.6, 147.2 (quinoline *C*H); 128.2, 131.7, 139.6 (quat $C_{quinoline}$). FAB$^+$-MS: *m*/*z* (%) 441 (100, (**1**)H$^+$), 248 (77, $C_{14}H_{10}NFe$). HR-MS (FAB$^+$): calcd for $C_{28}H_{21}N_2Fe$ 441.1054, found 441.1066. Anal. Calcd for $C_{28}H_{22}N_2FeCl_2\cdot 2CH_2Cl_2$: C, 52.75; H, 4.10; N, 3.84. Found: C, 53.30; H, 3.87; N, 4.58.

2·(HCl)$_2$ (8). A solution of **2** (90 mg, 0.19 mmol) in 20 mL of dichloromethane was treated with 1 mL of a saturated solution of hydrochloric acid in diethyl ether. The color changed from yellow to orange. After the mixture was stirred for 1 h, the solution was concentrated and filtered off and the orange precipitate was washed twice with dichloromethane and dried under vacuum: yield 100 mg (0.18 mmol, 97%). ^{1}H NMR (DMSO-d_6, 200.13 MHz): δ 4.90 (pt, 4H), 5.51 (pt, 4H), 7.15 (m, 2H), 7.52 (dd, ^3J(H,H) = 4.7 Hz, ^3J(H,H) = 8.3 Hz, 2H), 7.62 (dd, ^3J(H,H) = 7.4 Hz, ^4J(H,H) = 1.0 Hz, 2H), 7.75 (d, ^3J(H,H) = 8.2 Hz, ^4J(H,H) = 0.9 Hz, 2H), 8.46 (d, ^3J(H,H) = 8.2 Hz, ^4J(H,H) = 1.5 Hz, 2H), 8.86 (d, ^3J(H,H) = 4.7 Hz, ^4J(H,H) = 1.6 Hz, 2H), 10.9 (br, 2H). ^{13}C NMR (DMSO-d_6): δ 72.9, 74.3 (Cp *C*H); 86.4 (quat C_{Cp}); 121.3, 126.9, 127.5, 133.2, 142.9, 146.9 (quinoline *C*H); 128.1, 129.7, 138.2 (quat $C_{quinoline}$). FAB$^+$-MS: *m*/*z* (%) 487 (100, (**2**)H$^+$), 294 (36, $C_{14}H_{10}NRu$). HR-MS (FAB$^+$): calcd for $C_{28}H_{21}N_2{}^{102}Ru$ 487.0748, found 487.0724. Anal. Calcd for $C_{28}H_{22}N_2RuCl_2\cdot CH_2Cl_2$: C, 54.14; H, 3.76; N, 4.35. Found: C, 54.25; H, 4.09; N, 4.58.

X-ray Crystal Structure Determinations of 2−4, 6, 7a, and 8. Crystal data for **2**−**4**, **6**, **7a**, and **8** were collected on a Bruker AXS SMART 1000 diffractometer with a CCD area detector (Mo Kα radiation, graphite monochromator, λ = 0.710 73 Å) at −83 °C (**2**, **4**, **6**, **8**) and −100 °C (**3**, **7a**). An absorption correction (semiempirical from equivalents) was applied.[25] The structures were solved by direct methods and refined by full-matrix least squares against F^2 with all reflections using the SHELXTL programs.[26] All non-hydrogen atoms were refined anisotropically. All hydrogen atoms were located in difference Fourier maps and refined isotropically. Crystal data and experimental details are listed in Table 3.

Acknowledgment. We gratefully acknowledge the support of Prof. W. Siebert and the Deutsche Forschungsgemeinschaft (Sonderforschungsbereich 247). G.K. thanks the Landesgraduiertenförderung Baden-Württemberg for a scholarship.

Supporting Information Available: Tables giving X-ray crystal structure data for **2**−**4**, **6**, **7a**, **and 8**. This material is available free of charge via the Internet at http://pubs.acs.org.

OM010937O

(25) Sheldrick, G. M. SADABS, version 2.01; University of Göttingen, Göttingen, Germany, 2000.
(26) Sheldrick, G. M. SHELXTL NT, version 5.1; Bruker AXS, Madison, WI, 1999.